Prediction of flow resistance in a compound open channel

Mrutyunjaya Sahu, S. S. Mahapatra, K. C. Biswal and K. K. Khatua

ABSTRACT

Flooding in a river is a complex phenomenon which affects the livelihood and economic condition of the region. During flooding flow overtops the river course and spreads around the flood plain resulting in a two-course compound channel. It has been observed that the flow velocity in the flood plain is slower than that in the actual river course. This can produce a large shear layer between sections of the flow and produces turbulent structures which generate extra resistance and uncertainty in flow prediction. Researchers have adopted various numerical, analytical, and empirical models to analyze this situation. Generally, a one-dimensional empirical model is used for flow prediction assuming that the flow in the compound open channel is uniform. However, flow in a compound channel is quasi-uniform due to the transfer of momentum in sub-sections and sudden change of depths laterally. Hence, it is essential to analyze the turbulent structures prevalent in the situation. Therefore, in this study, an effort has been made to analyze the turbulent structure involved in flooding using large eddy simulation (LES) method to estimate the resistance. Further, a combination of an artificial neural network (ANN) and a fuzzy logic (FL) is considered to predict flow resistance in a compound open channel.

Key words | adaptive neuro-fuzzy inference system (ANFIS), compound open channel, computational fluid dynamics, correlation, momentum transfer

Mrutyunjaya Sahu
K. C. Biswal
K. K. Khatua
Department of Civil Engineering,
National Institute of Technology,
Rourkela,
Odisha,
India

S. S. Mahapatra (corresponding author)
Department of Mechanical Engineering,
National Institute of Technology,
Rourkela,
Odisha,
India
E-mail: *mahapatrass2003@yahoo.com*

INTRODUCTION

Resistance factors such as drag, boundary shear stress, and channel roughness play an important role in predicting conveyance capacity, bank protection, sediment transport, etc. Thus, Einstein & Banks (1950) and Krishnamurthy & Christensen (1972) developed models for estimating a composite friction factor to study resistance to the flow in a compound open channel. Wormleaton *et al.* (1982) reported through extensive experimentation that the Manning's equation and the Darcy–Weisbach equation are not suitable for predicting discharge of compound channels. Dracos & Hardegger (1987) proposed a model to predict a composite friction factor in compound open channel flow by taking momentum transfer into account, and they also noted that a composite friction factor depends on the main channel and flood plain widths and the ratio of the hydraulic radius to the depth in the main channel. Pang (1998) reported that the distribution of discharge between the main channel and flood plain is in accordance with the flow energy loss, which can be expressed in the form of a flow resistance coefficient. Christodoulou & Myers (1999) quantified the apparent shear on the vertical interface between main channel and flood plain in symmetrical compound sections. Yang *et al.* (2005) indicated that the Darcy–Weisbach resistance factor is not suitable for predicting a composite friction factor for measuring the resistance to flow. The environmental condition and the impact of thermodynamic, physical, and hydraulic parameters exhibit strong non-linear relationships leading to an inaccurate prediction of a composite friction factor in a compound open channel using conventional methods.

Rapid growth in artificial intelligent techniques not only reduces the tedious effort of experimentation but it also eliminates cumbersome computations. Walid & Shyam (1998) considered a back propagation (BP) algorithm of an

doi: 10.2166/hydro.2013.077

artificial neural network (ANN) for prediction of discharge in compound open channel flow. Notable past studies in this direction are a neuro-fuzzy model to simulate the Colebrook–White equation for the prediction of a friction factor in smooth open channel flow (Bigil & Altun 2008; Yuhong & Wenxin 2009) and the prediction of a friction factor in pipe flow problems (Fadare & Ofidhe 2009). Esen *et al.* (2008) demonstrated the use of adaptive neuro-fuzzy inference system (ANFIS) for modeling of a ground-coupled heat pump system. Riahi-Madvar *et al.* (2009) proposed a model based on ANFIS to predict longitudinal dispersion coefficient in natural streams. ANFIS has been adopted in a variety of fields for accurate prediction of responses in situations where input parameters characterize impreciseness and uncertainty. When the relationship between input and output parameters is difficult to establish using mathematical, analytical, and numerical methods and computation becomes cumbersome and time-consuming, an easily implementable technique like ANFIS can be adopted. Thus, an ANFIS model has been proposed in this study to predict a composite friction factor in compound open channel flow.

Despite clear successes in the experimental approach, it still suffers from limitations, such as: (i) data are collected at a limited number of points, (ii) the model is usually not at full-scale, and (iii) detailed measurements of turbulence have not usually been considered. A computational approach can partly overcome some of these issues and provide a complementary tool. In particular, a computational approach is readily repeatable, can simulate at full-scale and provides a spatially dense field of data points. However, there are significant technical challenges in terms of the prediction of turbulence. In recent years, numerical modeling of open channel flows has successfully reproduced experimental results. Computational fluid dynamics (CFD) has been used to model open channel flows ranging from main channels to full-scale modeling of flood plains. Simulations have been performed by Krishnappan & Lau (1986), Kawahara & Tamai (1988) and Cokljat (1993). CFD has also been used to model flow features in natural rivers by Sinha *et al.* (1998), Lane *et al.* (1999), and Morvan (2001). Thomas & Williams (1995a, 1995b, 1999) and Shi *et al.* (1999) have undertaken refined numerical modeling to examine the detailed time-dependent three-dimensional nature of flow to provide dense fields of data points. Further, they have adopted a large eddy simulation (LES) method to investigate over-bank channel flow. LES has been utilized to model both in-bank channel and over-bank flow condition to investigate the detailed structure of secondary circulations. Salvetti *et al.* (1997) conducted a LES simulation at a relatively large Reynolds number for producing results for bed shear with the magnitude of secondary motions and vorticity comparable to experiments. Pan & Banerjee (1995), Hodges & Street (1999), and Nakayama & Yokojima (2002) studied free surface fluctuations in open channel flow by employing the LES method where the free surface has been filtered along with the flow field itself which introduced extra sub-grid stress (SGS) terms. Beaman (2010) studied the estimation of conveyance using the LES method.

In this study, the inadequacy in prediction of a composite friction factor assuming turbulent flow and the momentum transfer between the main channel and flood plain is addressed using an adaptive neuro-fuzzy system. Further, keeping in view the wide application of LES in open channel flow, an effort has been made to analyze turbulent flow in a compound open channel.

EXPERIMENTAL DATA USED FOR ANALYSIS

The methods considered to predict the composite friction factor in a compound open channel are compared with the experimental data of FCF Series A (the experimental data for a straight compound open channel at the University of Birmingham) (Tominaga & Nezu 1991; Soong & DePue 1996; Tang & Knight 2001a, 2001b; Atabay *et al.* 2004). The hydraulic conditions of the data are shown in Table 1.

PREDICTION OF COMPOSITE FRICTION FACTOR BY ANFIS

Prediction of composite friction factor by empirical models

A compound channel basically consists of a main channel with flood plains. The primary factors affecting the

Table 1 | Summary of geometrical factors of experimental data

Source of data	Main side slope	Flood plain type	Roughness type	Main channel cross-sectional geometry
FCF Series A				
Series 1	1.0	Symmetric	Smooth	Trapezoidal
Series 2	1.0	Symmetric	Smooth	Trapezoidal
Series 3	1.0	Symmetric	Smooth	Trapezoidal
Series 6	1.0	Asymmetric	Smooth	Trapezoidal
Series 8	0	Symmetric	Smooth	Rectangular
Series 10	2.0	Symmetric	Smooth	Trapezoidal
Tominaga & Nezu (1991)				
S (1–3)	0	Asymmetric	Smooth	Rectangular
Tang & Knight (2001a)				
ROA	0	Symmetric	Smooth	Rectangular
ROS	0	Symmetric	Smooth	Rectangular
Tang & Knight (2001b)				
LOSR	0	Symmetric	Rough	Rectangular
ALL	0	Symmetric	Rough	Rectangular
Atabay *et al.* (2004)				
ROA	0	Asymmetric	Smooth	Rectangular
ROS	0	Symmetric	Smooth	Rectangular
Soong & Depue (1996)				
	1	Asymmetric	Rough	Trapezoidal

resistance coefficient in a compound open channel are geometric parameters (depth of main channel), h and the wall roughness resistant coefficient, $K = k_s/R$ where k_s and R are the roughness height and the hydraulic radius, respectively. It should be noted that the wall roughness changes along the wetted perimeter of the cross-section in a compound channel. The composite roughness on the wall as well as the shape of the channel affects the turbulent flow structures and the secondary current across the cross-section and hence, alters the resistance coefficient. Manning's equation is generally used for the prediction of discharge in compound open channels. The friction factor is in the form of either Manning's coefficient, Chezy's coefficient, or the Darcy–Weisbach coefficient, usually considered as a 'true composite friction factor' (Yang *et al.* 2007). In open channel flow, the flow resistance coefficient of the boundary expressed by Manning's coefficient (n), Chezy's coefficient (C), and Darcy–Weisbach (f) are related as shown in Equation (1):

$$\frac{C}{\sqrt{g}} = \frac{R^{1/6}}{\sqrt{g}} \times \frac{1}{n} = \frac{8}{\sqrt{f}} \tag{1}$$

These factors are evaluated to predict the bed shear stress and discharge for both simple and compound open channel flows. Traditionally, the composite roughness in a compound channel is expressed in Manning's form 'n' as in Equation (2). The composite friction factor n_c across the perimeter can be evaluated as:

$$n_c = \int w_i n_i dp \tag{2}$$

where n_i = sub-sectional Manning's roughness and w_i = weighted function of sub-sections. Using this formulation the calculation of open channel flow is reduced to a 1D formulation.

A number of empirical formulations have been proposed by investigators to predict a composite Manning's friction factor in compound open channel flow with different assumptions based on the relationships between the discharges, velocities, forces, and shear stresses of the component sub-sections and the total cross-section. These formulations are listed in Table 2 for the estimation of a composite Manning's friction factor. Further, different methods have been also adopted to divide the components sub-sections of the compound channels to apply these models to estimate a composite Manning's friction factor and the discharge in a compound open channel.

In this study, methods proposed by Cox (1973), Einstein & Banks (1950), Lotter (1933), Krishnamurthy & Christensen (1972), and Dracos & Hardegger (1987) have been adopted to predict a composite friction factor. Among these methods, only Dracos & Hardegger (1987) take momentum transfer into account. However, the model proposed by Hin *et al.* (2008) can account for momentum transfer but the method is based on field observation. Further, the data collected have to be calibrated to account for the shape factor parameter to calculate the apparent friction factor. Since this factor is not generally available, the model is excluded from this analysis. Figures 1–3 show the relationship between true composite friction factor obtained from Manning's

Table 2 | Models for prediction of composite Manning's friction factor

Reference	Model notation	Concept	Composite friction factor (n_c)
Cox (1973)	COX	Total resistance force is equal to sum of sub-area resistance forces or n_i weighted by $\sqrt{A_i}$	$= \sqrt{\sum n_i^2 \frac{A_i}{A}}$
		Total discharge is sum of sub-area discharges	$= \frac{A}{\sum (A_i/n_i)}$
Einstein & Banks (1950)	EBM	Total cross-sectional mean velocity equal to sub-area mean velocity	$= \left[\frac{\sum \left(n_i^{3/2} P_i\right)}{P}\right]^{2/3}$
Lotter (1933)	LM	Total discharge is sum of sub-area discharges	$= \frac{PR^{5/3}}{\sum \frac{P_i R_i^{5/3}}{n_i}}$
Krishnamurthy & Christensen (1972)	KCM	Logarithmic velocity distribution over depth h for wide channel	$= \exp\left[\frac{\sum P_i h_i^{3/2} \text{In } n_i}{\sum P_i \, h_i^{3/2}}\right]$
Dracos & Hardegger (1987)	D & H	The main channel and flood plain width ratio, and the ratio of the total hydraulic radius to the flow depth in the main channel	$\frac{n}{n_e} = f\left(\alpha, \frac{R}{H}\right)$

Where p_i = sub-sectional perimeter of compound channel, n_i = sub-sectional Manning's 'n', R_i = sub-sectional hydraulic radius, A_i = sub-sectional area of compound section, and h_i = sub-sectional depth of flow, R = hydraulic radius of whole compound channel, and α = a measure of increase in wetted perimeter.

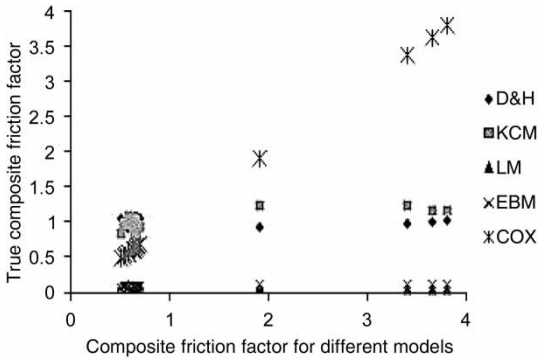

Figure 1 | True composite friction factor v/s composite friction factor predicted by five methods for Atabay *et al.*'s (2004) experimental conditions.

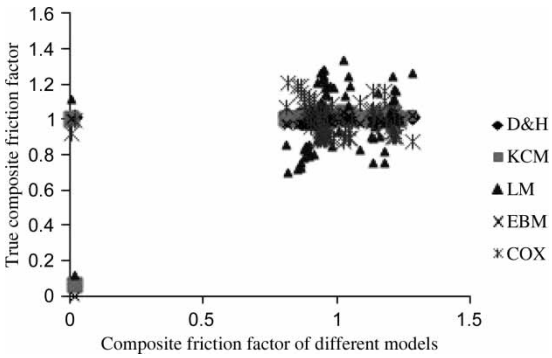

Figure 2 | True composite friction factor v/s composite friction factor predicted by five methods for Soong & Depue's (1996) experimental conditions.

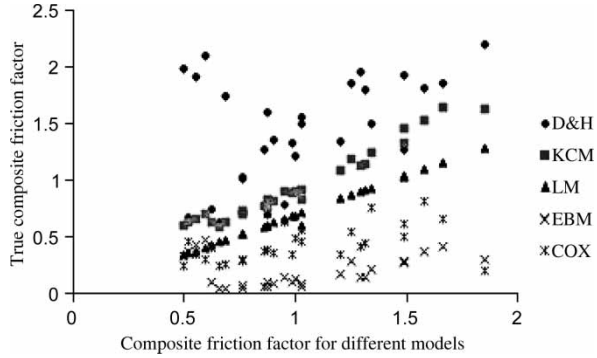

Figure 3 | True composite friction factor v/s composite friction factor predicted by five methods for Tang & Knight's (2001b) experimental conditions.

equation and the friction factor predicted by empirical models given in Table 2 for the three experimental conditions shown in Table 1. The mean absolute relative error for each model is shown in Table 3. It is inferred from Table 3 that the predictive models considered in this study are not capable of accurately predicting composite friction factor for all data sets. For example, Einstein & Banks' (1950) model predicts Soong & DePue's (1996) data with reasonable accuracy but fails to predict other data sets. Similarly, Krishnamurthy & Christensen's (1972) model predicts Tang & Knight's (2001a) data with adequate accuracy but no other data sets. Therefore, it is desirable to propose a robust predictive method

Table 3 | Mean absolute relative error for different data sets

Data set	Cox (1973)	Einstein & Banks (1950)	Lotter (1993)	Krishnamurthy & Christensen (1972)	Dracos & Hardegger (1987)
FCF Series A	28.33	32.6	24.16	49.47	15.738
Tominaga & Nezu (1991)	32.21	33.68	8.28	34.72	25.22
Tang & Knight (2001a)	28.81	57.58	13.52	9.37	13.74
Tang & Knight (2001b)	28.24	33.721	27.61	46.14	26.14
Atabay *et al.* (2004)	17.28	33.43	35.75	18.10	14.98
Soong & DePue (1996)	13.12	7.42	33.21	15.28	34.38

for an accurate prediction of a composite friction factor under different hydraulic conditions.

In order to develop a robust approach to predict a composite friction factor, five flow parameters used for the estimation of the overall discharge in compounds channels suggested by Yang *et al.* (2005) are considered. The parameters are: (i) relative width (B_r) (ratio of the width of the flood plain ($B - b$) to the total width (B) where b = main channel width); (ii) ratio of the perimeter of the main channel (P_{mc}) to the flood plain perimeter (P_{fp}) denoted as P_r; (iii) the ratio of hydraulic radius of the main channel (R_{mc}) to the flood plain (R_{fp}) denoted as R_r which usually varies with symmetry; (iv) the channel longitudinal slope (S_0); and (v) the relative depth (H_r) i.e., the flow depth of the flood plain ($H - h$) to the total depth (H) where h = main channel depth. In this study, these five flow parameters are chosen as input parameters and a composite friction factor as an output parameter.

Adaptive neuro-fuzzy inference system

The ANFIS is a combination of an ANN and a fuzzy inference system (FIS) where the neural network learns the structure of the data but understanding the network structure or the associated pattern is difficult. However, the FIS can understand the structure and develop the rule base using IF-THEN rules to predict the output. A neural network with its learning capabilities can be used to learn the fuzzy decision rules to create a hybrid intelligent system. The fuzzy system provides expert knowledge to be used by the neural network. A FIS consists of three components: first, a rule base which contains a selection of fuzzy rules; second, a database defines the membership functions used in the rules; and finally, a reasoning mechanism carries out the inference procedure on the rules and the given facts. Jang (1991a) proposed a combination of a neural network and fuzzy logic (FL) known as an ANFIS. ANFIS is a FIS implemented in the framework of neural networks. The combination of both ANN and FIS thus improves the system performance without interaction with operators. For this reason, it is possible to deduce the logical pattern of the prediction. The advantage of the technique is that the ANFIS architecture can be used to model the nonlinear functions for the prediction of the desired result in a logical manner (Jang 1991a, 1991b, 1993, 1994).

Fuzzy logic and fuzzy inference systems

Fuzzy systems are based on IF-THEN fuzzy rules. The building of FL systems begins with the derivation of a set of IF-THEN fuzzy rules comprising the expertise and knowledge of the modeling field (Dezfoli 2003). The modeling of suitable rules is tedious, and hence a predefined method or tool to achieve the fuzzy rules from numerical and statistical analysis is most appropriate for this context. Fuzzy conditional statements are expressed such as *if hydraulic depth (D_r) is small then friction factor is high* where these parameters are levels described by fuzzy sets that are characterized by membership functions. Hence, these concise forms of fuzzy rules are often employed to make decisions in situations of uncertainty. These play an important role in the human ability to make decisions.

From Figure 4, it can be observed that the FIS and fuzzy decision making procedure comprise five functional building blocks including: (i) rule base, (ii) database, (iii) decision making unit, (iv) fuzzification interface, and (v) defuzzification interface. The rule base and database are referred to as the knowledge base. The inference system is based on logical rules which map the input variables space to the output variable space using IF-THEN statements

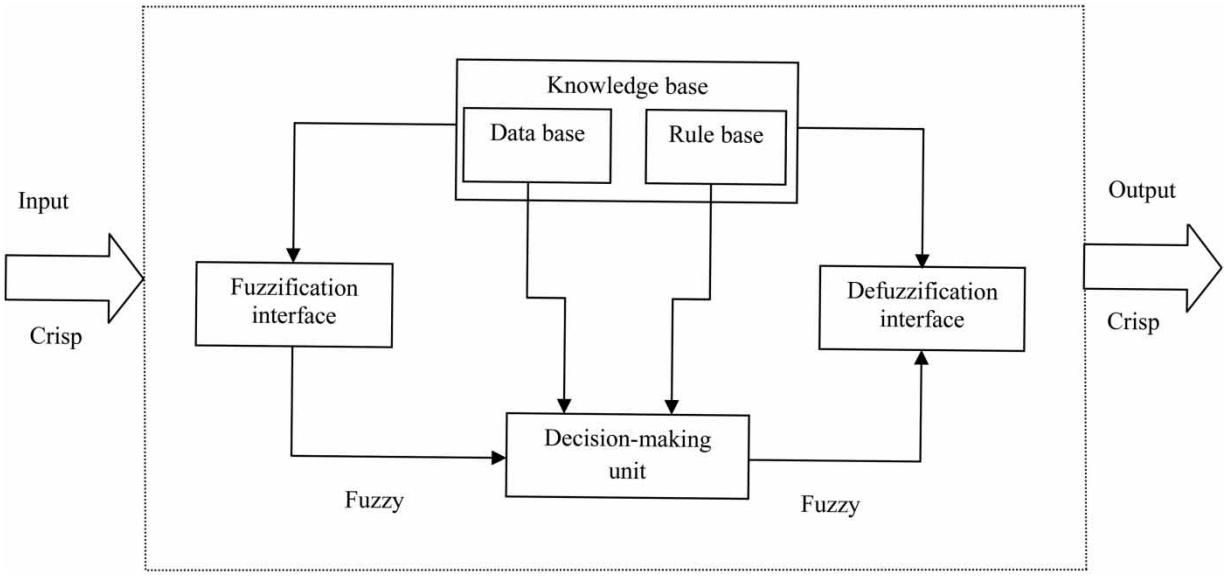

Figure 4 | Schematic diagram of fuzzy based inference system.

and a fuzzy decision making procedure (Dezfoli 2003; Jang & Gulley 1996). Due to the uncertainty of real and field values to fuzzy data, a fuzzification transition is used to transform deterministic values to fuzzy values and a defuzzification transition is used to transform fuzzy values into deterministic values (Dezfoli 2003).

Architecture and basic learning rules

A typical adaptive network shown in Figure 5 is a network structure consisting of a number of nodes connected through directional links. Each node is characterized by a node function with fixed or adjustable parameters. The learning or

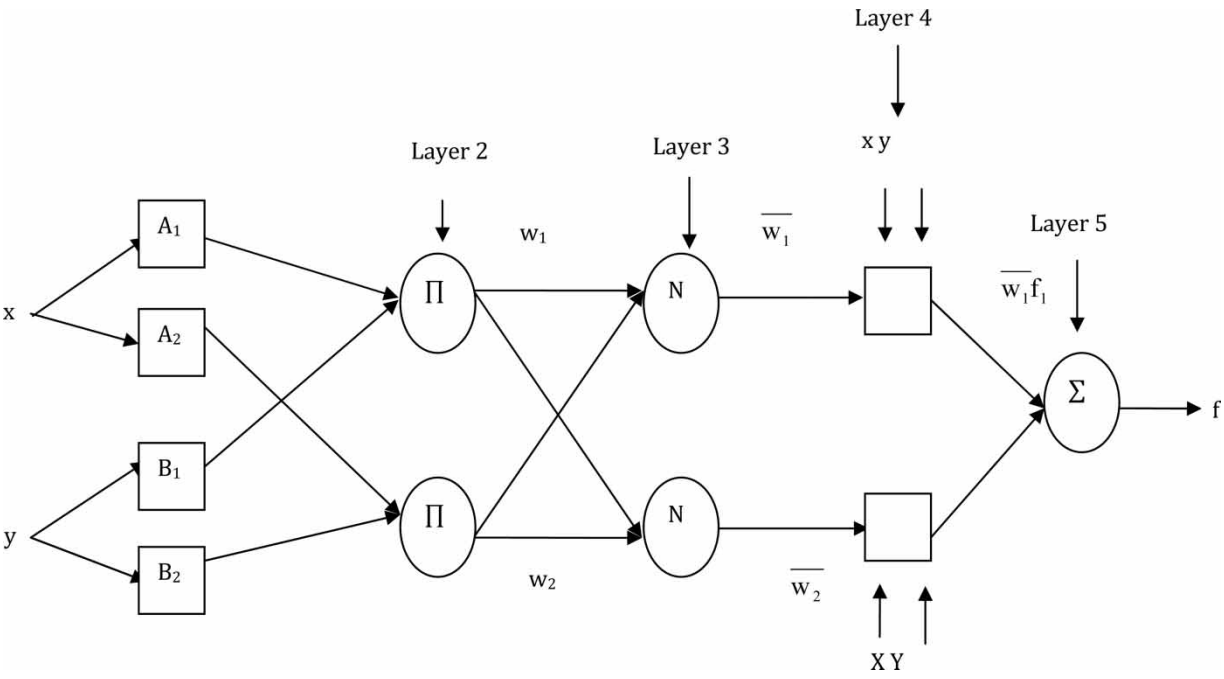

Figure 5 | A typical architecture of ANFIS system.

training phase of a neural network is a process to determine parameter values to sufficiently fit the training data. The basic learning rule method is the BP method which seeks to minimize some error, usually the sum of squared differences between the network's outputs and desired outputs. Generally, the model performance is checked by means of distinct test data, and a relatively good fit is expected in the testing phase. Considering a first order fuzzy interface system according to Takagi, Sugeno and Kang (TSK), a fuzzy model consists of two rules (Sugeno & Kang 1988):

$$\text{Rule 1: If } x \text{ is } A_1 \text{ and } y \text{ is } B_1 \text{ then } f_1 = p_1x + q_1y + r_1 \tag{3}$$

$$\text{Rule 2: If } x \text{ is } A_2 \text{ and } y \text{ is } B_2 \text{ then } f_2 = p_2x + q_2y + r_2 \tag{4}$$

If f_1 and f_2 are constants instead of linear equations, we have a zero order TSK fuzzy-model. Node functions in the same layer are of the same function family as described below. It is to be noted that O_i^j denotes the output of the i^{th} node in layer j.

Layer 1: Each node in this layer generates a membership grade of a linguistic label. For instance, the node function of the i^{th} node might be:

$$O_i^j = \mu A_i(x) = \frac{1}{1 + \left[\left(\frac{x - c_i}{a_i}\right)\right]^{b_i}} \tag{5}$$

where x is the input to the node i, and A_i is the linguistic label (small, large) associated with this node; and $\{a_i, b_i, c_i\}$ is the parameter set that changes the shapes of the membership function. Parameters in this layer are referred to as the 'premise parameters'.

Layer 2: Each node in this layer calculates the firing strength of each rule via multiplication:

$$O_i^2 = w_i = \mu A_i(x) \times \mu B_i(y), \; i = 1, 2 \tag{6}$$

Layer 3: The i^{th} node of this layer calculates the ratio of the i^{th} rule's firing strength to the sum of all rules' firing strengths:

$$O_i^3 = \overline{w_i} = \frac{w_i}{w_1 + w_2}, \; i = 1, 2 \tag{7}$$

For convenience outputs of this layer will be called normalized firing strengths.

Layer 4: Every node i in this layer is a squared node with a node function:

$$O_i^4 = \overline{w_i} f_i = \overline{w_i}(p_i + q_i y + r_i) \tag{8}$$

where $\overline{w}_i$ is the output of layer 3, and is the parameter set. Parameters in this layer will be referred to as 'consequent parameters'.

Layer 5: The single circle node computes the overall output as the summation of all incoming signals:

$$O_i^5 = \text{Overall output} = \sum_i^n \overline{w_i} f_i = \frac{\sum_i w_i f_i}{\sum_i w_i} \tag{9}$$

Thus, an adaptive network as presented in Figure 5 is functionally equivalent to a fuzzy interface. The basic learning rule of ANFIS is the BP gradient descent which calculates error signals (defined as the derivative of the squared error with respect to each node's output) recursively from the output layer backward to the input nodes (Werbos 1974). This learning rule is exactly the same as the back-propagation learning rule used in the common feed-forward neural networks (Rumelhart *et al.* 1986). From the ANFIS architecture (Figure 5), it is observed that given values of the premise parameters, the overall output can be expressed as a linear combination of the consequent parameters. Based on this observation, a hybrid learning rule is employed here, which combines a gradient descent and the least squares method to find feasible antecedent and consequent parameters (Jang 1991a, 1993). The details of the hybrid rule are given by Jang *et al.* (1997), where it is also claimed to be significantly faster than the classical back-propagation method.

Hybrid learning algorithm

From the ANFIS architecture (Figure 5), we observe that when the values of the premise parameters are fixed the overall output can be expressed as a linear combination. The output 'F' can be rewritten as:

$$\begin{aligned} F &= \frac{w_1}{w_1 + w_2} f_1 + \frac{w_1}{w_1 + w_2} f_2 \\ &= \overline{w} f_1 + \overline{w} f_2 \\ &= (\overline{w}x)p_1 + (\overline{w}y)q_1 + \overline{(w_1)}r_1 + (\overline{w_2}x)p_2 + (\overline{w_2}y)q_2 + (\overline{w_2})r_2 \end{aligned} \tag{10}$$

which is linear in the consequent parameters p_1, q_1, r_1, p_2, q_2, r_2. Therefore, the hybrid learning algorithm developed can be applied directly. More specifically, in the forward pass of the hybrid learning algorithm, node outputs go forward until layer 4 and the consequent parameters are identified by the least squares method. In the backward pass, the error signal propagates backward and the premise parameters are updated by gradient descent. As mentioned, the consequent parameters thus identified are optimal under the condition that the premise parameters are fixed. Accordingly, the hybrid approach converges much faster since it reduces the dimension of the search space of the original back-propagation method. This network fixes the membership functions and adapts only the consequent parts; then, ANFIS can be viewed as a functional-linked network (Klassen & Pao 1988; Pao 1989) where the enhanced representation, takes advantage of human knowledge and expresses more insight. By fine-tuning the membership functions, we actually generate this enhanced representation.

Training and testing of ANFIS network

The data required for the simulation are first generated using Manning's equation for obtaining a composite friction factor under different hydraulic conditions, as shown in Table 1. The input parameters for the simulation are referred to in a previous section (Prediction of composite friction factor by empirical models). The entire experimental data set is divided into training and testing data sets. A total of 228 data are used. Among the 228 data, 206 are considered as training data and 22 as testing data. The number of nodes in the second layer is increased gradually during the training process starting with two. It was observed that the error converges (decreases) as the nodes increase to five. Hence, the number of nodes in the second layer is fixed at five and further analysis is carried out. The five layers are one input, three hidden, and one output layer. The network was run on a MATLAB platform using a Pentium IV desktop computer. A Gaussian-type membership function (gauss2mf) is chosen for input as for input 1 and a linear-type membership function is used for output while generating FIS. The function goes steadily after 10 iterations due to a faster hybrid learning rule which ensured that the model parameters are matched. After that, 22 data are used for testing to verify the accuracy of the proposed model.

Prediction of composite friction factor using ANFIS

The composite friction factor is predicted using the ANFIS model based on five input parameters, such as relative width, ratio of perimeter of main channel to flood plain perimeter, ratio of hydraulic radius of main channel to flood plain, channel longitudinal slope, and relative depth. The pattern of variation of the actual and predicted composite friction factor is shown for the training and testing data sets in Figures 6 and 7, respectively. The black line indicates actual output and the grey line represents the predicted data from ANFIS. The plots show the coherent nature of the data distribution. The surface plot is shown in Figure 8. It can be observed that the surface covers the total landscape of decision space. Residuals are calculated as the difference between the actual and the predicted composite friction factors for training data set and are plotted in Figure 9. It can be observed that the residuals are distributed evenly along the centerline of the plot.

To verify the accuracy of the results, a regression analysis is also carried out. Regression curves are plotted in Figures 10 and 11 between the actual composite friction

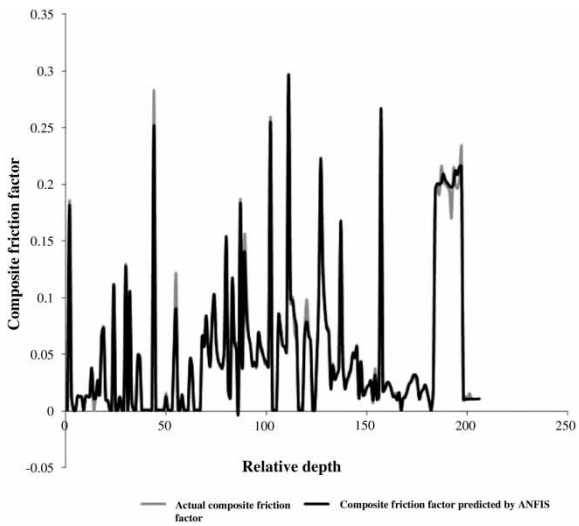

Figure 6 | Distribution of composite friction factor (training data).

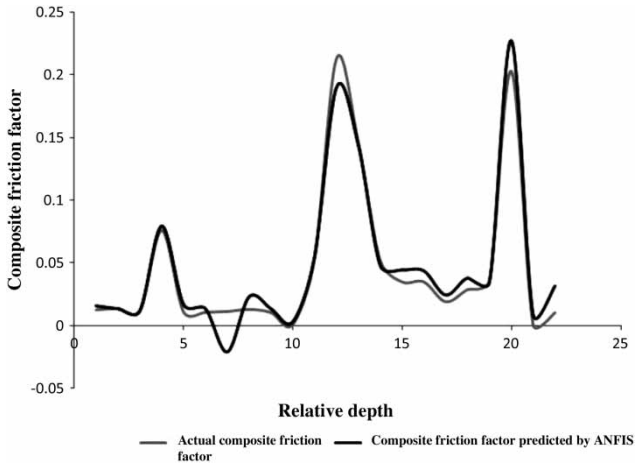

Figure 7 | Distribution of composite friction factor (testing data).

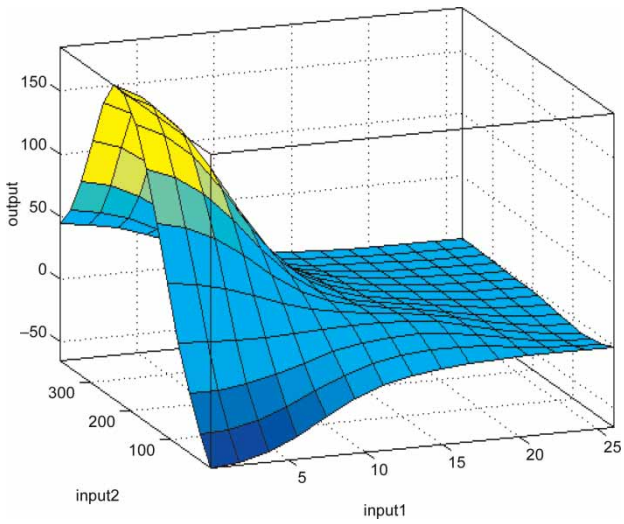

Figure 8 | Surface plot.

factor and the predicted composite friction factor for the training and the testing data, respectively. It can be observed that the data are well fitted because high values of the coefficient of determination ($R^2 = 0.991$ for training and $R^2 = 0.962$ for testing data) are obtained. The testing data set is used to find the coefficient of determination for the other five methods as shown in Figures 12–16. From these figures, it can be observed that the EBM method exhibits the least accuracy because the coefficient of determination (R^2) of EBM is 0.687 whereas the coefficient for the ANFIS method is 0.962.

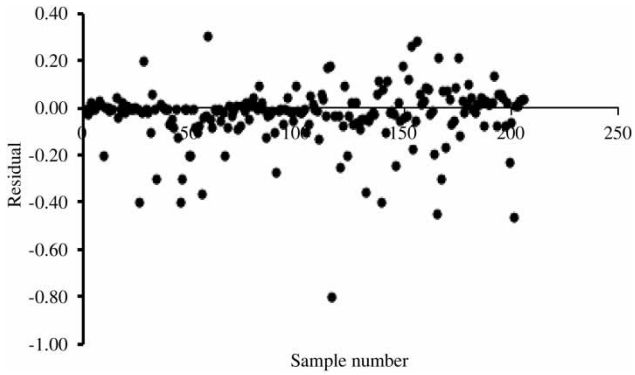

Figure 9 | Residual distribution of training data set.

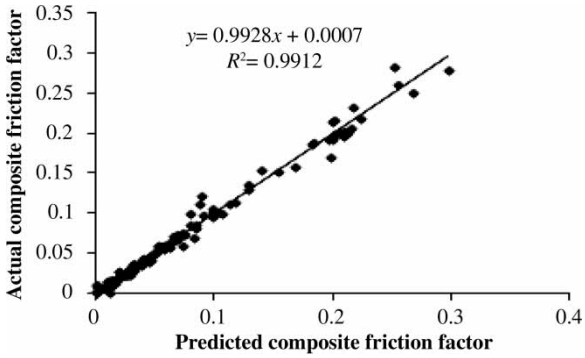

Figure 10 | Correlation plot for training set of data points.

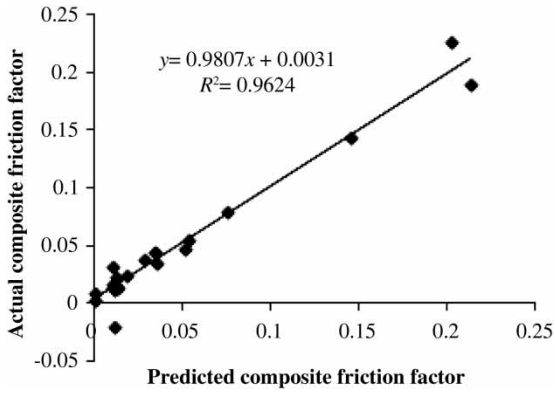

Figure 11 | Correlation plot for testing set of data points.

NUMERICAL MODELING OF TURBULENT FLOW STRUCTURES

Although the ANFIS model is quite robust in predicting a composite friction factor considering the non-linearity in the

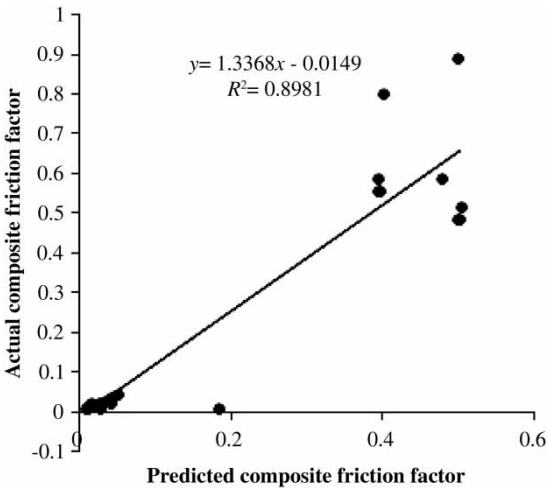

Figure 12 | Correlation plot for testing data (COX).

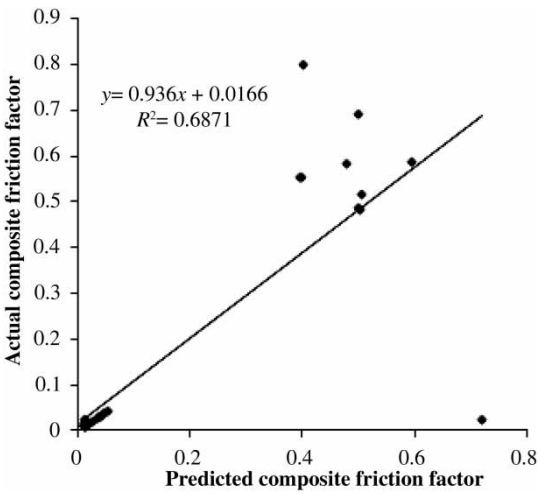

Figure 13 | Correlation plot for testing data (EBM).

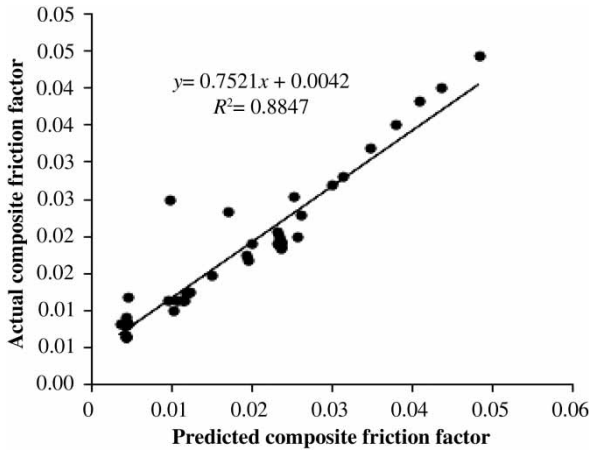

Figure 14 | Correlation plot for testing data (LM).

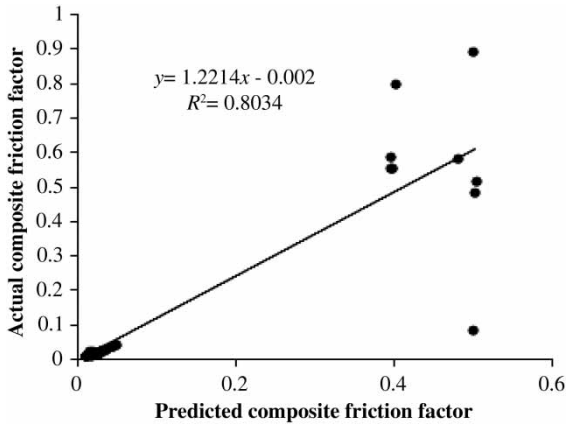

Figure 15 | Correlation plot for testing data (KCM).

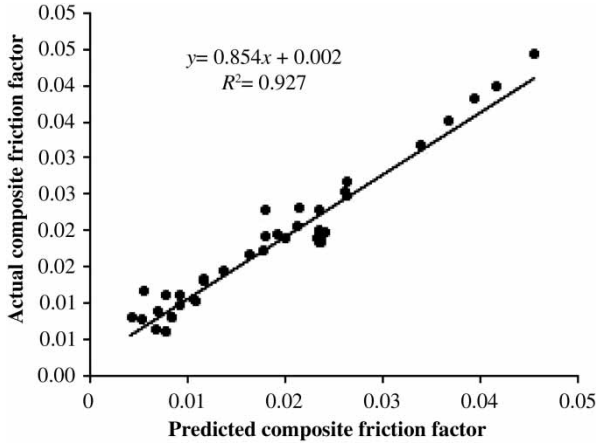

Figure 16 | Correlation plot for testing data (D & H).

relation between the input flow parameters and the output, it is vital to find out the reason for this non-linear relationship. In fact, momentum transfer in compound channels leads to an inaccurate estimation of discharge using empirical relations. Here, an attempt is made to present the effect of momentum transfer on the discharge in a compound channel via numerical analysis so that insight into flow mechanism can be gained. The numerical analysis simulates a tilting flume with a 8 m length and a $0.4 \times 0.4\ m^2$ cross-section for which Tominaga & Nezu (1991) carried out experiments using fiber-optic laser-Doppler anemometer to measure three-directional components of the turbulent velocity

shown in Figure 17 (S 1 case). The geometry of the channel is discretized with ANSYS 12 design modeler. The width to depth (B/H) ratio of the channel is 4.981 whereas the slope is 0.00064. The flow is considered as uniform incompressible turbulent flow at the test section 7.5 m from the inlet. The hydraulic radius (R) of the channel is 0.043. The Reynolds number (Re) of the flow for this case is 6.72×10^4.

The fluid flow equations are solved by discretizing the whole domain into unstructured hybrid mesh (mixture of prism and triangular) that divides the continuum into a finite number of nodes considering near-wall effect. The computations need a spatial discretization and time marching scheme. In this study, the transient simulation process is completed with the help of the commercial package ANSYS CFX (ANSYS CFX Tutorials ANSYS CFX Release 11.0 2006). This package generally solves the Navier–Stokes (NS) using a finite element-finite volume method. The mesh and simulation details are shown in Table 4. The governing equations (Equations (11) and (12)) are employed for LES obtained by filtering the time-dependent NS equation and continuity in either Fourier (wave-number) space or configuration (physical) space:

$$\frac{\partial \rho}{\partial t} + \frac{\partial(\rho \overline{u}_i)}{\partial x_i} = 0 \tag{11}$$

$$\frac{\partial}{\partial t}(\rho \overline{u}_i) + \frac{\partial(\rho \overline{u}_i \overline{u}_j)}{\partial x_i} = \frac{\partial}{\partial x_j}\left(\mu \frac{\partial \sigma_{ij}}{\partial x_j}\right) - \frac{\partial \overline{p}}{\partial x_i} - \frac{\partial \tau_{ij}}{\partial x_j} \tag{12}$$

where ρ = density of water, u_i and u_j are the unresolved velocity components in the x_i and x_j directions, σ_{ij} = normal stress in plane i along j direction, p = pressure, τ_{ij} = tangential shear stress in plane i along j direction. Equation (11) is the continuity equation which is linear and does not change due to filtering.

To capture the flow feature in turbulence, large-scale motion is captured as a direct numerical simulation (DNS) in LES but the effect of small scales is modeled using a subgrid scale (SGS) model. The LES method can incorporate a much coarser grid so that the temporal evolution of the large-scale turbulent motions can be directly simulated while the unresolved small-scale motions can be modeled

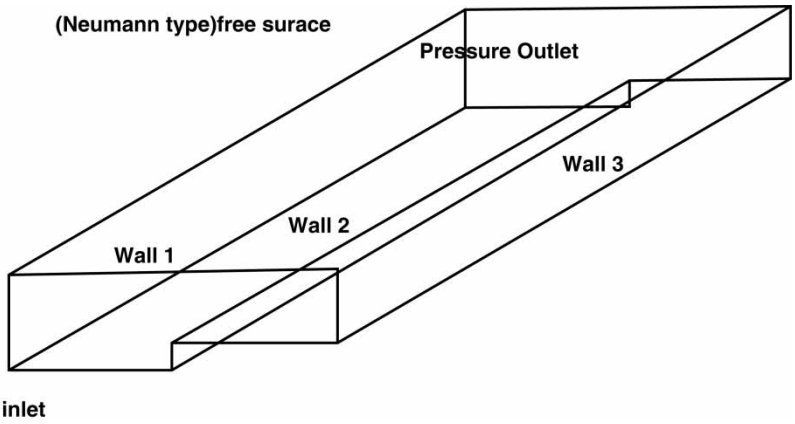

Figure 17 | Geometric alignment of flume channel along with boundary conditions.

Table 4 | Summary of mesh and simulation details using ANSYS-CFX

Case	Mesh spacing (m)	y^+ range	H/u^* (sec)	Time step (sec)	LETOT (Large eddy turn over time state) initial trial	
S 1	0.005	9.23–110.87	5	0.001	70	10

$y^+ = \frac{yu}{u^*}$ = scaled depth of flow where y = respective flow depth, u = flow velocity, u^* = shear velocity.

through the use of a Smagorinsky model. The filtering process filters out the eddies whose scales are smaller than the filter width or grid spacing used in the computations. The results of the simulation are compared with case S 1 of Tominaga & Nezu (1991). From Table 5, it is evident that the results obtained from LES simulation are in good agreement with case S 1 of Tominaga & Nezu (1991). Here, mean bulk velocity is calculated using the formulation:

$$W_b = \frac{\int w dA}{A} \tag{13}$$

where, W_b = mean velocity of the flow, w = velocity of the point of consideration.

The composite friction factor is calculated from Manning's equation.

The isovel lines of the non-dimensional stream-wise velocity $W(z)$ computed by the LES method are shown in Figure 18. The simulation shows that maximum velocity is 0.4049 m/s which is observed near the centerline of the channel at approximately 0.057 m from the centerline. The isovel lines bulge significantly upward in the vicinity of the junction edge along the flow. The patterns of the isovel lines from LES simulation results convincingly follow the experimental results of Tominaga & Nezu (1991). The reason for this bulge is the decelerated region on both sides of the junction region of the main channel. The region is created because of the low momentum transport due to the secondary current away from the wall. This causes the bulge in the main channel and flood plain interface due to high momentum transport by the secondary current. Consequently, the primary velocity is directly affected by the momentum transport due to the secondary current. The momentum transfer due to the secondary circulation component and the turbulent transport are three-dimensional in nature. These flow structures also depend on the corner of the channel and the shape of the compound cross-section. It is quite evident that turbulent structures as discussed are three-dimensional and highly non-linear.

Table 5 | Flow parameters of the experiment and simulation

Case	Maximum velocity, W_{max} (m/s)	Mean bulk velocity, W_b (m/s)	Composite friction factor, 'n_c'
S 1	0.409	0.368	0.011383
LES simulation results	0.4049	0.3671	0.011380

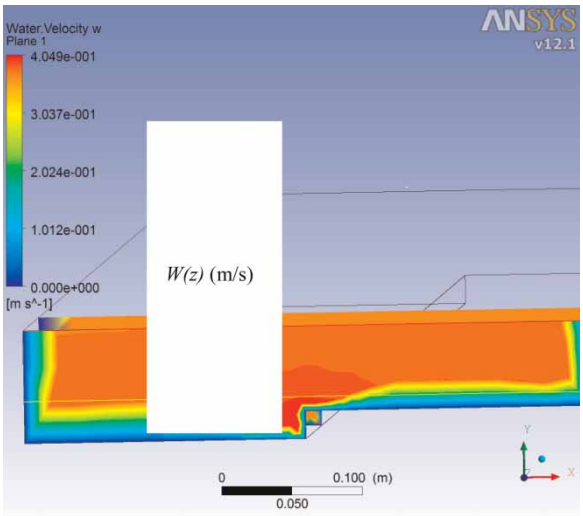

Figure 18 | Mean velocity distribution of LES simulation.

CONCLUSIONS

Based on analysis made in this study, the following certain conclusions can be drawn:

1. Five empirical models for the prediction of a composite friction factor have been studied. It is observed that the models can predict the composite friction factor accurately for a few data sets. Generally, the models break down when predicting the composite friction factor for a wide range of hydraulic conditions and geometries of compound channel.
2. To alleviate the above problem, a robust prediction strategy based on an ANFIS has been proposed. It is demonstrated that the ANFIS model is quite capable of predicting a composite friction factor with reasonable accuracy for a wide range of hydraulic conditions.
3. Further, the LES turbulence model has been adopted to analyze the compound open channel condition. The velocity distribution in an asymmetric compound channel is presented. The composite friction factor found from the LES is in good agreement with experimental results.

4. Moreover, both the LES and ANFIS models are fairly convincing and account for turbulence during the prediction of the discharge and the composite friction factor in a compound open channel. A reasonably accurate prediction of composite friction factor for different geometry, hydraulic conditions and bed/material can be obtained with less computational effort by ANFIS which can be useful for field engineers.
5. In future, the study can be extended to consider different hydraulic conditions for the prediction of composite friction factor using LES and ANFIS models.

REFERENCES

Atabay, S., Knight, D. W. & Seckin, G. 2004 Influence of a mobile bed on the boundary shear in a compound channel. In: *Proceedings of the Second International Conference on Fluvial Hydraulics*, Naples, Italy, 23–25 June, 1, pp. 337–345.

ANSYS CFX Tutorials ANSYS CFX Release 11.0. 2006 ANSYS Inc. Southpointe, 275 Technology Drive, Canonsburg, PA 15317.

Beaman, F. 2010 Large Eddy Simulation of Open Channel Flows for Conveyance Estimation. PhD Thesis, University of Nottingham.

Bigil, A. & Altun, H. 2008 Investigation of flow resistance in smooth open channels using artificial neural network. *Flow Meas. Instrum.* **19**, 404–408.

Christodoulou, G. C. & Myers, W. R. C. 1999 Apparent friction factor on the flood plain-main channel interface of compound channel sections. In: *Proc. 28th IAHR Congress*, Graz, Austria.

Cokljat, D. 1993 Turbulence Models for Non-circular Ducts and Channels. PhD Thesis, City University London.

Cox, R. G. 1973 Effective hydraulic roughness for channels having bed roughness different from bank roughness. Miscellaneous Paper H-73-2, US Army Engineers Waterways Experiment Station, Vicksburg, MS.

Dezfoli, K. A. 2003 *Principles of Fuzzy Theory and its Application on Water Engineering Problems*. Jihad Press, Tehran, Iran, p. 227.

Dracos, T. & Hardegger, P. 1987 Steady uniform flow in prismatic channels with flood plains. *J. Hydraul. Res. IAHR* **25** (2), 169–185.

Einstein, H. A. & Banks, R. B. 1950 Fluid resistance of composite roughness. *Trans. Am. Geo. Union* **31** (4), 603–610.

Esen, H., Inalli, M., Sengur, A. & Esen, M. 2008 Modeling a ground-coupled heat pump system using adaptive neuro-fuzzy inference systems. *J. Refrig.* **31** (1), 64–74.

Fadare, D. A. & Ofidhe, I. U. 2009 Artificial neural network model for prediction of friction factor in pipe flow. *J. Appl. Sci. Res.* **5** (6), 662–670.

Hin, L. S., Bessaih, N., Ling, L. P., Ghani, A., Zakaria, N. A. & Seng, M. Y. 2008 Discharge estimation for equatorial natural rivers with over bank flow. *Int. J. River Basin Manage.* **6** (1), 13–21.

Hodges, B. R. & Street, R. L. 1999 On simulation of turbulent nonlinear free-surface flows. *J. Comp. Phys.* **151**, 425–457.

Jang, R. J. 1991a Fuzzy modeling using generalized neural networks and Kalmman filter algorithm. In: *Int. Proc. 9th National Conf. on Artificial Intelligence*, Anaheim, CA, 15–19 July, pp. 762–767.

Jang, R. J. 1991b Rule extraction using generalized neural networks. In: *Int. Proc. 4th IFSA World Congress*, pp. 82–86.

Jang, R. J. 1993 ANFIS: adaptive-network-based fuzzy inference system. *IEEE Trans. Sys. Man. Cyber.* **23** (3), 665–685.

Jang, R. J. 1994 Structure determination in fuzzy modeling: a fuzzy CART approach. In: *Proc. IEEE conf. on Fuzzy Systems*, Orlando, FL.

Jang, J. S. R. & Gulley, N. 1996 *Fuzzy Logic Toolbox: Reference Manual*. The Math Works Inc., Natick, MA, USA.

Jang, J. S. R., Sun, C. T. & Mizutani, E. 1997 *Neuro-fuzzy and Soft Computing: A Computational Approach to Learning and Machine Intelligence.* Prentice-Hall International, London.

Kawahara, Y. & Tamai, N. 1988 Numerical calculation of turbulent flows in compound channels with an algebraic stress turbulence model. In: *Proc. 3rd Symp. Refined Flow Modeling and Turbulence Measurements*, Tokyo, Japan, pp. 9–17.

Klassen, M. S. & Pao, Y. H. 1988 Characteristics of the functional link net: a higher order delta rule net. In: *IEEE Proc. Conf. Neural Networks*, San Diego, CA.

Krishnamurthy, M. & Christensen, B. A. 1972 Equivalent roughness for Shallow channels. *J. Hydraul. Eng. ASCE* **98** (12), 2257–2263.

Krishnappan, B. G. & Lau, Y. L. 1986 Turbulence modeling of flood plain flows. *J. Hydraul. Eng. ASCE* **112** (4), 251–265.

Lane, S. N., Bradbrook, K. F., Richards, K. S., Biron, P. A. & Roy, A. G. 1999 The application of computational fluid dynamics to natural river channels: three-dimensional versus two-dimensional approaches. *Geomorphology* **29**, 1–20.

Lotter, G. K. 1993 Considerations on hydraulic design of channel with different roughness of walls. *Trans. AU Sci. Res. Inst. Hydraul. Eng.* **9**, 238–241.

Morvan, H. P. 2001 Three-dimensional Simulation of River Flood Flows. PhD Thesis, University of Glasgow, Glasgow.

Nakayama, A. & Yokojima, S. 2002 LES of open-channel flow with free-surface fluctuations. In: *Proc. Hydraul. Eng. JSCE*. **46**, 373–378.

Pan, Y. & Banerjee, S. 1995 Numerical investigation of free-surface turbulence in open-channel flows. *Phys. Fluids* **113** (7), 1649–1664.

Pang, B. 1998 River flood flow and its energy loss. *J. Hydraul. Eng. ASCE* **124** (2), 228–231.

Pao, Y. H. 1989 *Adaptive Pattern Recognition and Neural Network*. Addison-Wesley, Boston, MA, pp. 197–222.

Riahi-Madvar, H., Ayyoubzadeh, A. S., Khadangi, E. & Ebadzadeh, M. M. 2009 An expert system for predicting

longitudinal dispersion coefficient in natural streams by using ANFIS. *Exp. Sys. App.* **36** (2), 1142–1154.

Rumelhart, D. E., Hinton, G. E. & William, D. E. 1986 Learning internal representations by error propagation. In: *Parallel distributed processing: explorations in the microstructure of cognition* (D. E. Rumelhart & J. L. McClelland, eds). MIT Press, Cambridge, MA, pp. 318–362.

Salvetti, M. V., Zang, Y., Street, R. L. & Banerjee, S. 1997 Large-eddy simulation of free-surface decaying turbulence with dynamic subgrid-scale models. *Phys. Fluids* **9** (8), 2405–2419.

Shi, J., Thomas, T. G. & Williams, J. J. R. 1999 Large eddy simulation of flow in a rectangular open channel. *J. Hydraul. Res.* **37** (3), 345–361.

Sinha, S. K., Sotiropoulos, F. & Odgaard, A. J. 1998 Three-dimensional numerical model for flow through natural rivers. *J. Hydraul. Eng.* **124** (1), 13–24.

Soong, T. W. & DePue II, P. M. 1996 Variation of Manning's Coefficient with Channel Stage. Unpublished MS Thesis, University of Illinois at Urbana-Champaign, Urbana, IL.

Sugeno, M. & Kang, G. T. 1988 Structure identification of fuzzy model. *Fuzzy Sets Syst.* **28**, 15–33.

Tang, X. & Knight, D. W. 2001a Analysis of bed form dimensions in a compound channel. In: *Proceedings of 2nd IAHR Symposium on River, Coastal and Estuarine Morphodynamics*, Obihiro, Japan, pp. 555–563.

Tang, X. & Knight, D. W. 2001b Experimental study of stage-discharge relationships and sediment transport rates in a compound channel. In: *Proc. 29th IAHR Congress*, Beijing, China, 16–21 September, pp. 69–76.

Thomas, T. G. & Williams, J. 1995a Large eddy simulation of a symmetric trapezoidal channel at Reynolds number of 430,000. *J. Hydraul. Res.* **33** (6), 825–842.

Thomas, T. G. & Williams, J. 1995b Large eddy simulation of turbulent flow in an asymmetric compound open channel. *J. Hydraul. Res.* **33** (1), 27–41.

Thomas, T. G. & Williams, J. 1999 Large eddy simulation of flow in a rectangular open channel. *J. Hydraul. Res.* **37** (3), 345–361.

Tominaga, A. & Nezu, I. 1991 Turbulent structures in compound open-channel flow. *J. Hydraul. Eng. ASCE* **117**, 21–41.

University of Birmingham Flow Database. Available at: www.flowdata.bham.ac.uk/atabay/index.shtml; www.flowdata.bham.ac.uk/fcfa.shtml; www.flowdata.bham.ac.uk/tang/data.shtml.

Walid, H. S. & Shyam, S. S. 1998 An artificial neural network for non-iterative calculation of the friction factor in pipeline flow. *Comput. Electron. Agric.* **21**, 219–228.

Werbos, P. J. 1974 Beyond Regression: New Tools for Prediction and Analysis in the Behavioral Sciences. Dissertation, Harvard University, Cambridge, MA.

Wormleaton, P. R., Allen, J. & Hadjipanos, P. 1982 Discharge assessment in compound channel flow. *J. Hydraul. Eng. ASCE* **108** (9), 975–994.

Yang, K., Cao, S. & Liu, X. 2005 Study on resistance coefficient in compound channels. *Acta Mech. Sinica* **21**, 353–361.

Yang, K., Cao, S. & Liu, X. 2007 Flow resistance and its prediction methods in compound channels. *Acta Mech. Sinica* **23**, 23–31.

Yuhong, Z. & Wenxin, H. 2009 Application of artificial neural network to predict the friction factor of open channel. *Commun. Nonlinear Sci. Numer. Simulat.* **14**, 2373–2378.

First received 10 April 2012; accepted in revised form 1 May 2013. Available online 30 May 2013